https://doi.org/10.5194/angeo-2021-46
Preprint. Discussion started: 17 August 2021

Annales Geophysicae Discussions

Automatic calculation of the magnetometer zero offset using the interplanetary magnetic field based on the Wang-Pan method

Xiaowen Hu[1], Guoqiang Wang[2], Zonghao Pan[1], Tielong Zhang[1, 2,]

[1]Chinese Academy of Sciences Key Laboratory of Geospace Environment, School of Earth and Space Sciences, University of Science and Technology of China, Hefei 230026, China;

[2]Institute of Space Science and Applied Technology, Harbin Institute of Technology, Shenzhen, China

Correspondence: Guoqiang Wang (wanggq@hit.edu.cn)

Abstract

The space-borne fluxgate magnetometer (FGM) needs regular in-flight calibration to obtain its zero offset. Recently, a new method based on the properties of Alfvén waves for the zero offset calibration was developed by Wang and Pan (2021). They found that there exists an optimal offset line (OOL) in the offset cube for a pure Alfvén wave, and the zero offset can be determined by the intersection of at least two non-parallel OOLs. Since no pure Alfvén waves exist in the interplanetary magnetic field, the calculation of the zero offset relies on the selection of the highly Alfvénic fluctuation event. Here, we propose an automatic procedure to find highly Alfvénic fluctuations in the solar wind and calculate the zero offset. This procedure includes three parts: (1) selection of highly Alfvénic fluctuation events, (2) evaluation of the OOL of the selected fluctuation events, and (3) determination of the zero offset. We test our automatic procedure by applying it to the magnetic field data measured by the FGM onboard Venus Express. The tests reveal that our automatic procedure is able to achieve as good results as the Davis-Smith method. One advantage of our procedure is that the selection criteria and process for the highly Alfvénic fluctuation event are simpler. Our automatic procedure might also be applied to find fluctuation events for the Davis-Smith method after proper

https://doi.org/10.5194/angeo-2021-46
Preprint. Discussion started: 17 August 2021

Annales Geophysicae
Discussions
Open Access

modification.

https://doi.org/10.5194/angeo-2021-46
Preprint. Discussion started: 17 August 2021

Annales Geophysicae
Discussions

1. Introduction

There are abundant dynamic processes in the space plasma environment, such as reconnections (Zhang et al., 2012; Lu et al., 2020), instabilities (Hellinger et al., 2017; Duan et al., 2018), turbulences (Huang et al., 2018; Xiao et al., 2020a, 2020b), linear magnetic holes (Ge et al., 2011; Wang et al., 2020, 2021a), and magnetohydrodynamic waves (Keiling, 2008; Wang et al., 2015, 2016, 2017). Some kinetic-scale processes or structures require the accurate measurement of the magnetic field (Burch et al., 2016; Wang et al., 2021b). Therefore, the high-precision magnetic field measurement is crucial to investigate the physical processes in space.

The fluxgate magnetometer (FGM) is one of the most widely used instruments for detecting the magnetic field in space (Acuña, 2002; Balogh, 2010; Burch et al., 2016; Liu et al., 2020). In order to accurately measure the magnetic field, the FGM needs to be calibrated before the launch of the spacecraft (Olsen et al., 2003; Risbo et al., 2003). Nevertheless, regular in-flight calibration is still needed to perform since its instrumental offset, the value measured in a null field environment, varies slowly with time (Balogh, 2010; Olsen et al., 2003). In addition, the slowly changing (or static) magnetic field generated by the spacecraft at the sensor position is generally not negligible, and it is difficult to distinguish the static magnetic field from the instrumental offset (Pope et al., 2011; Pudney et al., 2012). Thus, both the static magnetic field and the instrumental offset are regarded as the zero offset of the space-borne FGM (Leinweber et al., 2008). Alfvén waves (Davis and Smith, 1968; Belcher, 1973; Hedgecock, 1975) as well as mirror mode structures (Plaschke and Narita, 2016; Plaschke et al., 2017; Plaschke, 2019; Schmid et al., 2020) can be used to calculate the zero offset.

Based on the properties of Alfvén waves, the Davis-Smith method (Davis and Smith, 1968), the Becher method (Belcher, 1973), and the Hedgecock method (Hedgecock, 1975) have been proposed to calculate the zero offset. Both the Becher method and

https://doi.org/10.5194/angeo-2021-46
Preprint. Discussion started: 17 August 2021

Hedgecock method require a long time interval (a few days or longer) of input data, which makes these two methods not suitable for the in-flight calibration of the spacecraft partially orbiting in the solar wind, such as Venus Express (Zhang et al., 2006) and the Magnetospheric Multiscale (MMS) mission (Russell et al., 2016). Leinweber et al. (2008) found that the Davis-Smith method is mathematically superior to the other two methods and needs a much shorter time interval of input data, and the accuracy of the zero offset calculation depends on the selection of the interplanetary magnetic field (IMF) fluctuations.

Recently, a new method has been proposed by Wang and Pan (2021) to calculate the zero offset of the FGM based on properties of the Alfvén wave. For the convenience of description, we refer to this new method as the Wang-Pan method. Wang and Pan (2021) found that the zero offset **O** is on a straight line determined by an Alfvén wave event in the offset cube, and the authors defined this line as the optimal offset line (OOL). They also found that the intersection of at least two non-parallel OOLs determined by different Alfvén waves can be used to determine the zero offset. The Wang-Pan method can deal with the IMF fluctuation with a duration less than 1 minute, and it calculates the zero offset more intuitive. However, Wang and Pan (2021) did not provide a method or criterion to select the IMF fluctuation to perform the Wang-Pan method.

In this study, we develop an automatic procedure to search out the highly Alfvénic IMF fluctuation and then calculate the zero offset based on the Wang-Pan method. We first briefly introduce the Wang-Pan method in section 2. Then, we give the details of the automatic procedure in section 3. In section 4, we apply this automatic procedure to perform the in-flight calibration of the FGM onboard the Venus Express spacecraft. Section 5 presents the summary of our work.

2. Wang-Pan method

Alfvén waves do not change the magnetic field strength (Keiling, 2008). Based on

https://doi.org/10.5194/angeo-2021-46
Preprint. Discussion started: 17 August 2021

such a property of Alfvén waves, Wang and Pan (2021) found that there exists an OOL with good linearity in the offset cube, and this line passes through the real zero offset. The range of each side of the offset cube can be set according to the possible range of the IMF strength, which is typically less than 20 nT. The intersection of at least two non-parallel OOLs resulting from different Alfvén waves is expected to be the zero offset.

2.1 Optimal offset line

Now we introduce the definition of the OOL and how to obtain the OOL of an Alfvén wave in the offset cube (Wang and Pan, 2021). We assume that the sensitivities and non-orthogonality angles of the FGM have been calibrated except for the zero offset $\mathbf{O}$ (= (O_X, O_Y, O_Z)), thereby the magnetic field data $\mathbf{B}_M$ (= (B_{M_X}, B_{M_Y}, B_{M_Z})) is only composed of the natural magnetic field $\mathbf{B}_A$ (= (B_{A_X}, B_{A_Y}, B_{A_Z})) and $\mathbf{O}$, or $\mathbf{B}_M = \mathbf{B}_A + \mathbf{O}$. Since the typical value of the IMF strength is < 20 nT, the three components of $\mathbf{O}$ are expected to be in the range of ($\langle B_{M\_X}\rangle - 20$, $\langle B_{M\_X}\rangle + 20$), ($\langle B_{M\_Y}\rangle - 20$, $\langle B_{M\_Y}\rangle + 20$) and ($\langle B_{M\_Z}\rangle - 20$, $\langle B_{M\_Z}\rangle + 20$) nT, respectively, where $\langle B_{M\_X}\rangle$, $\langle B_{M\_Y}\rangle$ and $\langle B_{M\_Z}\rangle$ are the average values of the three components of $\mathbf{B}_M$. Thus, an offset cube in the same coordinate system of $\mathbf{B}_M$ can be built and the three axes of this offset cube are in the ranges of ($\langle B_{M\_X}\rangle - 20$, $\langle B_{M\_X}\rangle + 20$), ($\langle B_{M\_Y}\rangle - 20$, $\langle B_{M\_Y}\rangle + 20$) and ($\langle B_{M\_Z}\rangle - 20$, $\langle B_{M\_Z}\rangle + 20$) nT, respectively. One can found that the zero offset is a certain point in this offset cube.

The magnetic field data are modified to be $\mathbf{B}'_M = \mathbf{B}_A + \mathbf{O} - \mathbf{O}'$ at the point $\mathbf{O}'$ in the offset cube. To find out which point in the offset cube is the zero offset, Wang and Pan (2021) tried to find the point which is most likely to be the zero offset in each parallel plane. For a pure Alfvén wave, the standard deviation δ of $\mathbf{B}'_M$ is zero when $\mathbf{O} = \mathbf{O}'$, and δ is non-zero when $\mathbf{O} \neq \mathbf{O}'$. Therefore, Wang and Pan (2021) optimized the point in each parallel plane that is most likely to be the zero offset by minimizing the value of δ in the corresponding plane. And they find that these points in the corresponding parallel

https://doi.org/10.5194/angeo-2021-46
Preprint. Discussion started: 17 August 2021

planes are approximately on a straight line, which is defined as the OOL, because any point on this line could be the zero offset. Furthermore, the OOL is parallel to the vector $(\langle B_{A\_X}\rangle, \langle B_{A\_Y}\rangle, \langle B_{A\_Z}\rangle)$, where $\langle B_{A\_X}\rangle$, $\langle B_{A\_Y}\rangle$ and $\langle B_{A\_Z}\rangle$ are the averages of the three components of $\mathbf{B}_A$, respectively.

The physical meaning of the OOL can be better understood in the mean field-aligned (MFA) coordinate system. In this coordinate system, the z-axis is parallel to the ambient magnetic field, and the fluctuation of the Alfvén wave is only in the x-y plane. Thus, the strength of the magnetic field in the x-y plane $\sqrt{B_x^2 + B_y^2}$ is a constant (Keiling, 2008; Wang et al., 2015). In the offset cube, the non-constant value of the modified magnetic field strength in the x-y plane is expected to be caused by the x and y components of $\mathbf{O} - \mathbf{O}'$. Thus, in the offset cube, we can obtain the x and y components of zero offset in MFA. However, the z component of the zero offset could be any value. Thus, we cannot determine the zero offset just based on a single Alfvén wave. The most likely values of the zero offset in MFA form a straight line parallel to the z-axis, and this line is the so-called OOL.

2.2 Determination of the zero offset

To find out the zero offset $\mathbf{O}$, at least two non-parallel OOLs are necessary. As shown in Figure 1, the intersection of the three non-parallel OOLs is the zero offset, since all the OOLs pass through the point $\mathbf{O}$ in the offset cube.

https://doi.org/10.5194/angeo-2021-46
Preprint. Discussion started: 17 August 2021

Annales Geophysicae Discussions
Open Access

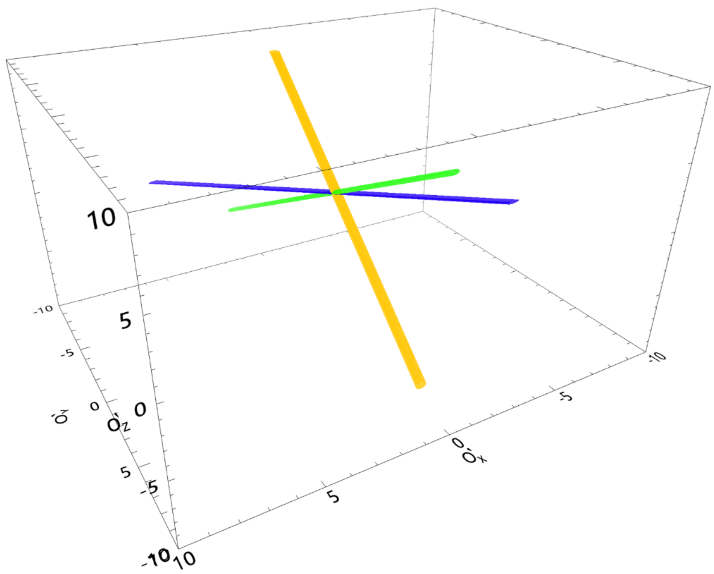

Figure 1. Schematic of the zero offset determined by three non-parallel OOLs in the offset cube.

Due to the influence of the compressional wave and the magnetic field noise, even if the corresponding IMF fluctuation event has a highly Alfvénic nature, the OOL is usually not a straight line. Anyway, the point that minimize δ in each plane can be fitted into a straight line, which is called the fitted optimal offset line (FOOL). The FOOL usually does not pass the zero offset point, resulting in no common intersection for the non-parallel FOOLs in the offset cube. Therefore, Wang and Pan (2021) optimized the zero offset so that the sum of the distances from the point in the offset cube to all the FOOLs determined by different IMF fluctuation events is smallest.

3. Automatic procedure

For the Wang-Pan method, the process of determining the zero offset can be simplified as finding the point in the offset cube that minimizes the sum of the distances from this point to all the non-parallel FOOLs (Wang and Pan, 2021). It is easy to obtain the zero offset based on the Wang-Pan method when we obtain the IMF fluctuation events with a highly Alfvénic nature. Therefore, finding such IMF fluctuation events

https://doi.org/10.5194/angeo-2021-46
Preprint. Discussion started: 17 August 2021

automatically is the key to achieve automatic calculation of the zero offset. Here, we develop an automatic procedure to calculate the zero offset using the IMF fluctuations based on the Wang-Pan method. This automatic procedure consists of three parts: (1) selection of the highly Alfvénic fluctuation events, (2) evaluation of the OOL for each event, and (3) calculation of the zero offset.

The magnetic field data measured by the FGM onboard the Venus Express (VEX) spacecraft is used to illustrate the implementation of our automatic procedure. The VEX spacecraft, launched on 9 November 2005, is a three-axis stabilized spacecraft (Titov et al., 2006). VEX is the first mission of Europe to Venus, and one of its main scientific objectives is to study the solar wind interaction with Venus (Zhang et al., 2006). The VEX FGM measured the magnetic field with a sampling rate up to 128 Hz using two triaxial fluxgate sensors. The ambient natural magnetic field and the dynamic field generated by the spacecraft can be separated based on the dual-sensor configuration (Zhang et al., 2006; Pope et al., 2011). In this study, we use the 1 Hz data of VEX FGM in the spacecraft coordinate system to calculate the zero offset. Except for the zero offset, the sensitivities and non-orthogonal angles of the FGM have been calibrated, so the data we used are called partially calibrated data.

3.1 Selection of the highly Alfvénic fluctuation event

There are rich of magnetic field fluctuations and structures in the solar wind, such as Alfvén waves (Li et al., 2016; Wu et al., 2016), mirror mode structures (Volwerk et al., 2021; Wang et al., 2021a), and discontinuities (Artemyev et al., 2019; Neukirch et al., 2020). We need to select the magnetic field fluctuation with a highly Alfvénic nature from the partially calibrated data.

Figure 2 shows the partially calibrated magnetic field data in the spacecraft coordinate system between 00:00 UT on 1 January and 12:00 UT on 2 January 2007. Based on the bow shock model (Shan et al., 2015) and the location of the VEX spacecraft, the VEX spacecraft is confirmed to be in the solar wind as shown in the gray area of Figure 2. The magnetic field fluctuations have the following characteristics: (1) they do not have a fixed period, and the periods of the fluctuations vary from a few seconds to several hundred seconds; (2) the amplitude is dominant in different components of the magnetic field during different intervals; (3) after removing the zero offset, the transverse component of the magnetic field fluctuations dominates in some intervals, while the compressional component dominates in other intervals.

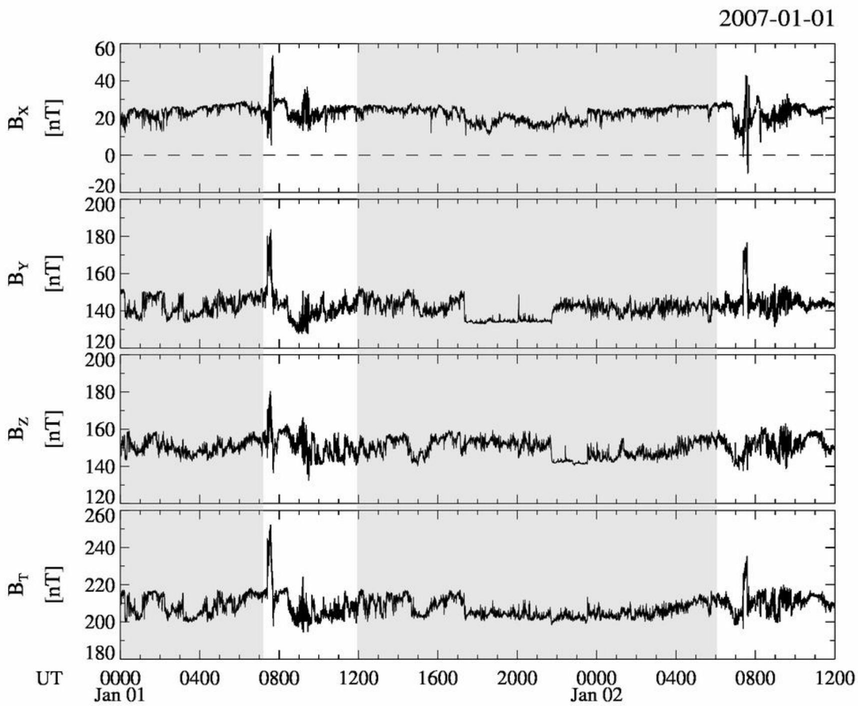

Figure 2. The partially calibrated magnetic field data of VEX in the spacecraft coordinate system and its strength between 00:00 UT on 1 January 2007 and 12:00 UT on 2 January 2007. The gray area denotes the VEX spacecraft is in the solar wind.

The selection of the highly Alfvénic fluctuation event can be divided into two steps: first, selection of the start and end moments of the event, and second, evaluation of the event's Alfvénic nature. Since the IMF has strong variations with periods typically less than 5 minutes as shown in Figure 2, we only select the IMF fluctuation events with

https://doi.org/10.5194/angeo-2021-46
Preprint. Discussion started: 17 August 2021

periods within 5 minutes. To find the start and end time of a fluctuation event, the following procedures are executed in parallel on the three components of magnetic field data:

(i). To reduce the effect of the high-frequency noise of the data, the 10 s boxcar filter is used to smooth the data of each component, and the result is marked as B_{i_sm1} (the index i represents the component X, Y, or Z of FGM in this procedure). To obtain the ambient magnetic field, the 200 s boxcar filter is used to smooth the data of each component, and marked as B_{i_sm2}.

(ii). We find all the moments when the value of B_{i_sm1}- B_{i_sm2} is 0, and the collection of these moments is marked as T_i. The first moment in T_i, marked as T_{i_0}, is regarded as the start time of the fluctuation event. The end moment T_{i_1} of this fluctuation event is also in the collection of T_i determined according to the following criteria: a) 30 s < $T_{i\_1} - T_{i\_0}$ < 10 min, and b) the number of the elements in T_i is in the range of 2 – 5. When the above two criteria are met at the same time, the number of T_i should be as large as possible.

(iii). Calculate the standard deviation δ_i of each magnetic field component in the period determined by start time T_{i_0} and end time T_{i_1}.

(iv). We can obtain three periods after the above steps. The period corresponding to the maximum standard deviation δ_i is determined as the period of the fluctuation event eventually.

(iv). The end time of this event is selected as the start time of the next event. We repeat the steps (i) ~ (iv) until we get the start and end time of all fluctuation events in the solar wind in each VEX orbit.

According to the Wang-Pan method (Wang et al., 2021) introduced in section 2, we first build an offset cube in the same coordinate system as $\mathbf{B_M}$, and the three axes of the offset cube are in the range of $(\langle B_{A\_X}\rangle - 20, \langle B_{A\_X}\rangle + 20)$, $(\langle B_{A\_Y}\rangle - 20, \langle B_{A\_Y}\rangle + 20)$ and $(\langle B_{A\_Z}\rangle - 20, \langle B_{A\_Z}\rangle + 20)$ nT, respectively. At the point $\mathbf{O}'$ in the offset cube, the magnetic field is modified as $\mathbf{B}'_A = \mathbf{B_M} - \mathbf{O}'$. For a fluctuation event with a highly

https://doi.org/10.5194/angeo-2021-46
Preprint. Discussion started: 17 August 2021

Alfvénic nature, the standard deviation of the total field strength is generally very small. Thus, the standard deviation $\delta_{B'_T}$ of $|\mathbf{B}'_A|$ is expected to be very small at a certain point in the offset cube when the real ambient magnetic field B_A is a fluctuation event with a highly Alfvénic nature. We calculate the values of $\delta_{B'_T}$ in the offset cube with a step length of 0.1 nT along each axis. If the minimum value of $\delta_{B'_T}$ is < ξ_1 (here, ξ_1 is set to be 0.1 nT) in the offset cube, we identify the fluctuation event as a highly Alfvénic fluctuation event.

Figure 3 shows an example of selecting the fluctuation event using the partially calibrated data of the VEX spacecraft between 04:00 and 05:00 UT on 1 January 2007. The red curves indicate the three components of the ambient magnetic field. The gray areas in Figure 3 indicate the automatically selected highly Alfvénic fluctuation events with different periods. One can find that our above procedures can obtain the interval of a fluctuation event with different temporal scales.

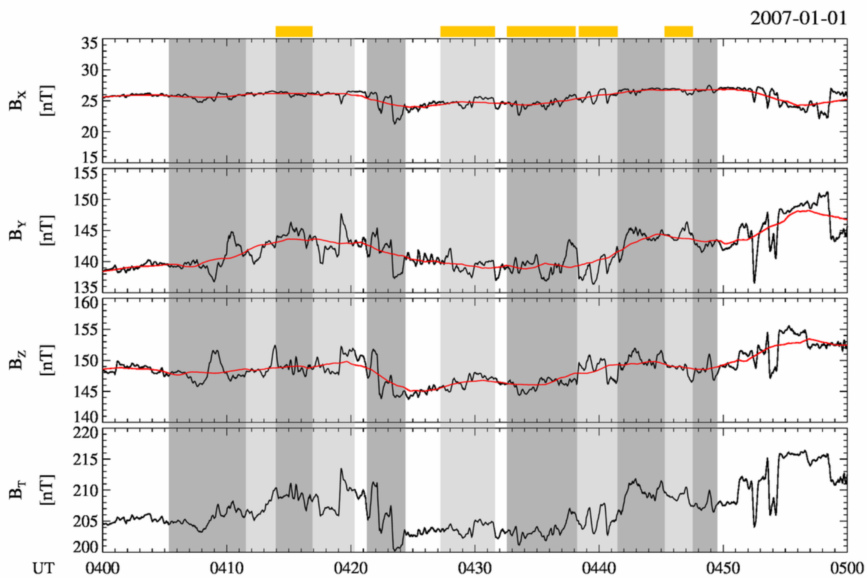

Figure 3. The VEX partially calibrated magnetic field data between 04:00 and 05:00 UT on 1 January 2007. The red curve denotes the ambient magnetic field $\mathbf{B}_{A\_sm2}$. The gray area denotes the

https://doi.org/10.5194/angeo-2021-46
Preprint. Discussion started: 17 August 2021

interval of the selected fluctuation event, and the yellow tag denotes the interval of the selected highly Alfvénic fluctuation event.

3.2 Evaluation of the OOL for each event

After obtaining the highly Alfvénic fluctuation events, we then need to determine the OOLs of these events. The OOL is expected to be a straight line for a pure Alfvén wave (Wang and Pan, 2021). Due to the effect of the compressional fluctuation, the OOL is usually not a straight line even for a highly Alfvénic fluctuation event (Wang and Pan, 2021). Besides, the OOL with a high linearity cannot be obtained if the normal direction of the plane is not selected properly for some events. Since we cannot know in advance which axis is the best choice to be the normal direction of the reference plane to obtain the minimum $\delta_{B_T'}$, we use the following steps to obtain the OOL:

(i). We find the points of P_{OX} (= [P_{OX_X}, P_{OX_Y}, P_{OX_Z}]) which are the minima of $\delta_{B_T'}$ in the planes perpendicular to the O_X' axis with a step of $\Delta O_X'$ = 1 nT. Note that the P_{OX} cannot be located at the boundary of the plane. We require that the number of P_{OX} is not less than 10. Then we calculate the correlation coefficients between P_{OX_X} and P_{OX_Y}, P_{OX_X} and P_{OX_Z}, and P_{OX_Y} and P_{OX_Z} respectively. The maximum absolute value among these coefficients is noted as R_{OX}. Similarly, we can obtain the sets of points P_{OY} and P_{OZ}, and their corresponding correlation coefficients R_{OY} and R_{OZ}.

(ii). If R_{OX} is larger than R_{OY} and R_{OZ}, and R_{OX} is > r (here, r = 0.9), then P_{OX} is selected to be the OOL. Similarly, P_{OY} or P_{OZ} can also be selected as the OOL when the R_{OY} or R_{OZ} is the maximum of the three correlation coefficients and is > r. If R_{OX}, R_{OY}, and R_{OZ} are all < 0.9, the corresponding event will not be selected to calculate the zero offset.

(iii). We then obtain the FOOL of the OOL determined in step (ii).

(iv). Repeat the steps (i) ~ (iv) until we get the FOOLs of all the selected highly Alfvénic fluctuation events which meet the requirements in the (i) and (ii) steps.

Figure 3 displays 8 highly Alfvénic fluctuation events as shown in the gray areas. We

https://doi.org/10.5194/angeo-2021-46
Preprint. Discussion started: 17 August 2021

use the above procedure to further select the events whose OOLs have good linearity. As the yellow tags shown in Figure 3, only 3 out of 8 events meet the above criteria for good linearity.

3.3 Calculation of zero offset

The FOOL is expected to be parallel to the ambient magnetic field and passes through the zero offset in the offset cube for a pure Alfvén wave (Wang and Pan, 2021). Due to the effect of the compressional fluctuation, the FOOL does not pass through the zero offset. Therefore, Wang and Pan (2021) optimize the zero offset so that the sum of the distances from the point to all the FOOLs is the smallest. We use the following steps to determine the zero offset:

(i). In the section 3.2, we obtain the FOOLs in the time period during which the FGM needs in-flight calibration. We select N adjacent FOOLs to determine the zero offset. Here, the number N is set to be 16. We require that all these FOOLs are within 1 day.

(ii). We obtain the distance L from the point O' to the FOOL in the offset cube. In order to reduce the influence of a certain FOOL deviating far from the estimated zero offset, we convert the distance L to be a probability f(L), and $f(L) = \frac{1}{\sqrt{2\pi}\delta}\exp\left(-\frac{L^2}{2\delta^2}\right)$. Here, we set the standard deviation $\delta = 3$ nT. We determine the zero offset to be the point in the offset cube so that the sum of the values of f(L) resulting from all the FOOLs is the largest. The average time of these FOOLs are considered to be the time of the estimated zero offset.

(iii). We use any N – 1 out of the N FOOLs to determine the zero offset using the method described in the step (ii), then we can obtain N estimated zero offsets. The maximum and minimum of these N zero offsets can be used to evaluate the calculation error of the zero offset determined by the N FOOLs.

(iv). We repeat the steps (i) ~ (iii) to determine the zero offset of the next N FOOLs whose sequence number is shifted by M until all the FOOLs have been used to determine the zero offset. Here, M is set to be 1.

https://doi.org/10.5194/angeo-2021-46
Preprint. Discussion started: 17 August 2021

Annales Geophysicae Discussions
Open Access

Figure 4 shows an example of the calculation of the zero offset using 16 highly Alfvénic fluctuation events observed by VEX on 1 January 2007. Figure 4A shows the FOOLs of the 16 events as well as their time intervals. As shown by the dots, one can find that the linearity of the OOL is high for each event. The red triangle in Figure 4B denotes the zero offset $\mathbf{O}_1$ (= [16.88, 142.73, 151] nT) determined by the automatic procedure introduced in this section, and the blue dot denotes the zero offset $\mathbf{O}_2$ determined by any 15 out of the 16 events. The X, Y, and Z components of $\mathbf{O}_2$ are in the ranges of [16.8, 17.11], [142.66, 142.83], and [150.87, 151.13] nT, respectively. The minimum and maximum of $\mathbf{O}_2$ can be used to evaluate the calculation error of $\mathbf{O}_1$.

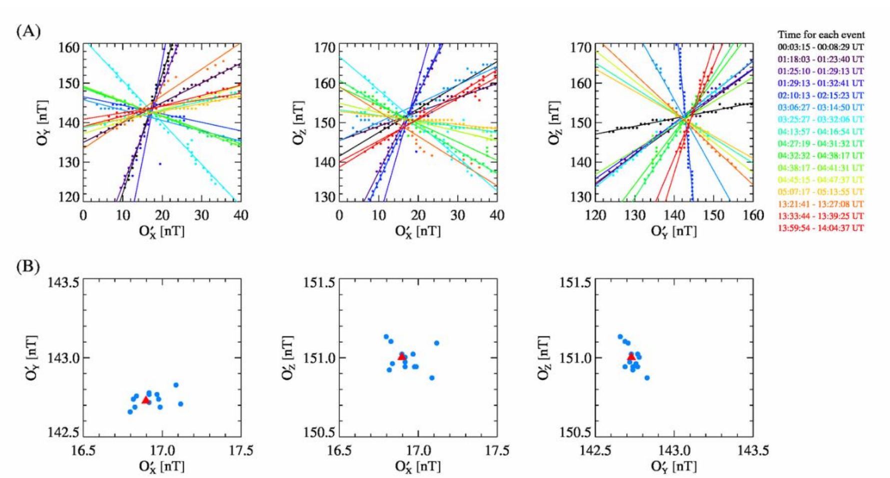

Figure 4. (A) The FOOLs (solid lines) for the 16 highly Alfvénic fluctuation events observed by VEX on 1 January 2007. Each dot denotes the position of the minimum $\delta_{B'_T}$ in the corresponding plane for a certain event. The time intervals of the 16 events are also given. (B) The zero offset determined by the FOOLs. The red triangle denotes the zero offset determined by the 16 events. The blue dot denotes the zero offset determined by any 15 out of 16 events.

4. Application to VEX

We apply our automatic procedure to the partially calibrated data of VEX from January 1, 2007 to March 31, 2007. Based on the location of the VEX spacecraft and the model of the Venusian bow shock (Shan et al., 2015), we first find the time intervals during which the VEX spacecraft was in the solar wind. Then, the data are used to

https://doi.org/10.5194/angeo-2021-46
Preprint. Discussion started: 17 August 2021

Annales Geophysicae
Discussions
Open Access

determine the zero offset based on the automatic procedure described in section 3. The zero offsets determined by our procedure are shown by the red dots in Figure 5. We also determine the zero offset using the Davis-Smith method with the same fluctuation events, and the results are shown by the blue dots in Figure 5. For comparison, Figure 5 also displays the zero offset provided by the VEX FGM team as shown by the orange triangles, and each day has one estimated zero offset. One can find that the profiles of the red, blue dots, and orange triangles are very similar, suggesting that our automatic procedure is successful to get a reliable results of zero offset.

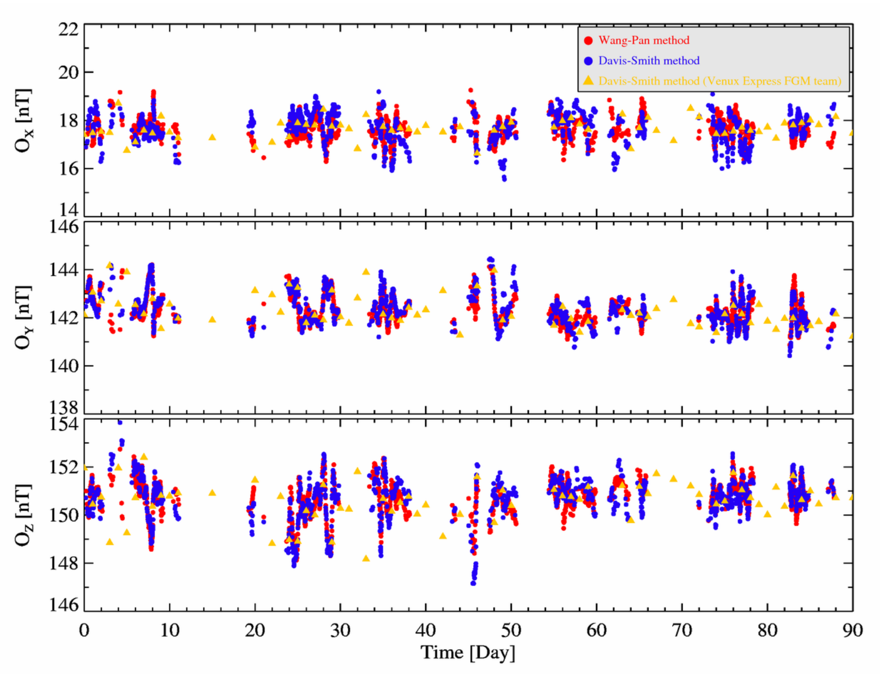

Figure 5. The zero offset for the VEX partially calibrated magnetic field data from 1 January 2007 to 31 March 2007. The red (blue) dot denotes the zero offset determined by the Wang-Pan (Davis-Smith) method. The orange triangle denotes the zero offset provided by the MAG team of the VEX spacecraft.

Figure shows the difference between the zero offsets determined by the Wang-Pan method and the Davis-Smith method using the highly Alfvénic fluctuation events

https://doi.org/10.5194/angeo-2021-46
Preprint. Discussion started: 17 August 2021

selected by our automatic procedure. ΔO is marked as the difference of the zero offsets determined by the two methods. About 64.2% values of ΔO_X are within [-0.5, 0.5] nT, and the corresponding probabilities of ΔO_Y and ΔO_Z are 87.2% and 73.9%. It suggests that the calculation results of the Wang-Pan method are very close to those of the Davis-Smith method when using the same fluctuation events selected by our automatic procedure.

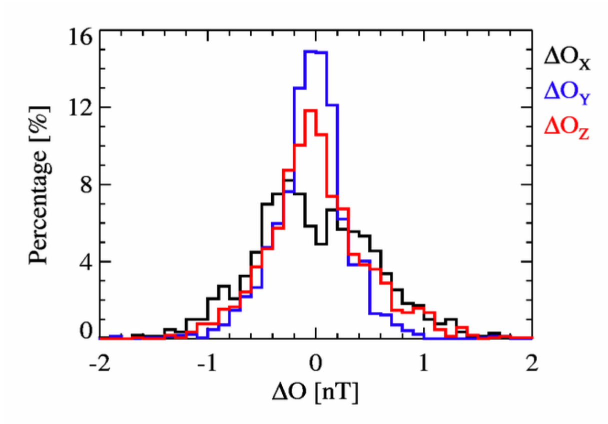

Figure 6. The distribution of the difference between the zero offsets determined by the Wang-Pan method and the Davis-Smith method.

5. Summary

In order to make the application of the Wang-Pan method more convenient, we develop an automatic procedure to automatically find the fluctuation events of highly Alfvénic nature in the solar wind and determine the zero offset of the FGM. This automatic procedure consists of three parts: (1) selection of the highly Alfvénic fluctuation event, (2) obtaining the OOL with good linearity for the fluctuation event, and (3) determination of the zero offset using at least two non-parallel OOLs. We test our automatic procedure by using three months of the partially calibrated data measured by VEX FGM, and find that our automatic procedure is successful to achieve as good results as the Davis-Smith method.

https://doi.org/10.5194/angeo-2021-46
Preprint. Discussion started: 17 August 2021

Since both the Wang-Pan method and the Davis-Smith method are based on the properties of Alfvén waves (Davis and Smith, 1968; Wang and Pan, 2021), the selection of fluctuation events with a highly Alfvénic nature is critical for both methods. Thereby, Leinweber et al. (2008) provided the following three selection criteria for the application of the Davis-Smith method: (1) the first criterion is designed to require the fluctuation in each data window to lie at least within a single plane; (2) the second criterion requires that the magnetic field has a low level of compression after being calibrated; (3) the third criterion requires that each magnetic field component has no strong correlation with the recalculated magnetic field strength. For the Wang-Pan method, we also need to select the highly Alfvénic fluctuation events, and the criteria for selecting highly Alfvénic fluctuation events can be summarized into the following two simple criteria: (1) the minimum of the standard deviations of the modified magnetic field strength in the offset cube should be small enough; (2) the OOL should have good linearity. One can find that these two selection criteria are more intuitive.

Our automatic procedure is developed based on the two criteria of the Wang-Pan method, and consists of three parts: selection of the potentially high Alfvénic fluctuation events, evaluation of the OOLs, and determination of the zero offset. The purpose of the first two parts is to select the highly Alfvénic fluctuation event. After the highly Alfvénic fluctuation events have been selected, we can choose either the Wang-Pan method or the Davis-Smith method to calculate the zero offset (Leinweber et al., 2008; Wang and Pan, 2021). As shown in Figure 5, these two methods can achieve very similar results. Therefore, our automatic procedure can also be used to automatically calculate the zero offset based on the Davis-Smith method after a slight modification.

https://doi.org/10.5194/angeo-2021-46
Preprint. Discussion started: 17 August 2021

Acknowledgements.

This work in China was supported by NSFC grants 41804157, 41774171, 41774167, 41974205, 41804157 and 41904156. The authors also acknowledge the financial support from the pre-research Project on Civil Aerospace Technologies (No. D020103) funded by CNSA, the 111 project (B18017), CAS Center for Excellence in Comparative Planetology, and Macau foundation. We thank Professor Tielong Zhang for providing the partially calibrated magnetic field data of the Venus Express.

https://doi.org/10.5194/angeo-2021-46
Preprint. Discussion started: 17 August 2021

Annales Geophysicae Discussions Open Access EGU

References

Acuña, M. H. (2002), Space-based magnetometers, Review of Scientific Instruments, 73(11), 3717-3736, doi:10.1063/1.1510570.

Artemyev, A. V., Angelopoulos, V., Vasko, I. Y., Runov, A., Avanov, L. A., Giles, B. L., et al. (2019), On the Kinetic Nature of Solar Wind Discontinuities, Geophysical Research Letters, 46(3), 1185-1194, doi:10.1029/2018gl079906.

Balogh, A. (2010), Planetary Magnetic Field Measurements: Missions and Instrumentation, Space Science Reviews, 152(1-4), 23-97, doi:10.1007/s11214-010-9643-1.

Belcher, J. W. (1973), Variation of Davis-Smith Method for in-Flight Determination of Spacecraft Magnetic-Fields, Journal of Geophysical Research, 78(28), 6480-6490, doi:DOI 10.1029/JA078i028p06480.

Burch, J. L., Moore, T. E., Torbert, R. B., & Giles, B. L. (2016), Magnetospheric Multiscale Overview and Science Objectives, Space Science Reviews, 199(1-4), 5-21, doi:10.1007/s11214-015-0164-9.

Davis, L., & Smith, E. J. (1968), The in-flight determination of spacecraft magnetic field zeros, EOS Transaction American Geophysical Union, 49, 257.

Duan, A. Y., Zhang, H., & Lu, H. Y. (2018), 3D MHD simulation of the double-gradient instability of the magnetotail current sheet, Science China-Technological Sciences, 61(9), 1364-1371, doi:10.1007/s11431-017-9158-7.

Ge, Y. S., McFadden, J. P., Raeder, J., Angelopoulos, V., Larson, D., & Constantinescu, O. D. (2011), Case studies of mirror-mode structures observed by THEMIS in the near-Earth tail during substorms, Journal of Geophysical Research-Space Physics, 116(A1), doi:10.1029/2010ja015546.

Hedgecock, P. C. (1975), A correlation technique for magnetometer zero level determination, Space Science Instrumentation, 1(1), 83–90.

Hellinger, P., Landi, S., Matteini, L., Verdini, A., & Franci, L. (2017), Mirror Instability in the Turbulent Solar Wind, The Astrophysical Journal, 838(2), doi:10.3847/1538-4357/aa67e0.

Huang, S. Y., Sahraoui, F., Yuan, Z. G., Le Contel, O., Breuillard, H., He, J. S., et al. (2018), Observations of Whistler Waves Correlated with Electron-scale Coherent Structures in the Magnetosheath Turbulent Plasma, Astrophysical Journal, 861(1), doi:10.3847/1538-4357/aac831.

Keiling, A. (2008), Alfvén Waves and Their Roles in the Dynamics of the Earth's Magnetotail: A Review, Space Science Reviews, 142(1-4), 73-156, doi:10.1007/s11214-008-9463-8.

Leinweber, H. K., Russell, C. T., Torkar, K., Zhang, T. L., & Angelopoulos, V. (2008), An advanced approach to finding magnetometer zero levels in the interplanetary magnetic field, Measurement Science and Technology, 19(5), doi:10.1088/0957-0233/19/5/055104.

Li, H., Wang, C., Chao, J. K., & Hsieh, W. C. (2016), A new approach to identify interplanetary Alfven waves and to obtain their frequency properties, Journal of Geophysical Research-Space Physics, 121(1), 42-55, doi:10.1002/2015ja021749.

Liu, K., Hao, X., Li, Y., Zhang, T., Pan, Z., Chen, M., Hu, X., Li, X., Shen, C., & Wang, Y. (2020), Mars Orbiter magnetometer of China's First Mars Mission Tianwen-1, Earth and Planetary Physics, 4(4), 384-389, doi:10.26464/epp2020058.

Lu, S., Wang, R. S., Lu, Q. M., Angelopoulos, V., Nakamura, R., Artemyev, A. V., et al. (2020), Magnetotail reconnection onset caused by electron kinetics with a strong external driver, Nature Communications, 11(1), doi:10.1038/s41467-020-18787-w.

Neukirch, T., Vasko, I. Y., Artemyev, A. V., & Allanson, O. (2020), Kinetic Models of Tangential Discontinuities in the Solar Wind, Astrophysical Journal, 891(1), doi:10.3847/1538-4357/ab7234.

Olsen, N., Toffner-Clausen, L., Sabaka, T. J., Brauer, P., Merayo, J. M. G., Jorgensen, J. L., et al. (2003), Calibration of the Orsted vector magnetometer, Earth Planets and Space, 55(1), 11-18, doi:10.1186/Bf03352458.

Plaschke, F., & Narita, Y. (2016), On determining fluxgate magnetometer spin axis offsets from mirror mode observations, Annales Geophysicae, 34(9), 759-766, doi:10.5194/angeo-34-759-2016.

Plaschke, F., Goetz, C., Volwerk, M., Richter, I., Fruhauff, D., Narita, Y., et al. (2017), Fluxgate magnetometer offset vector determination by the 3D mirror mode method, Monthly Notices of the Royal Astronomical Society, 469(Suppl_2), S675-S684, doi:10.1093/mnras/stx2532.

Plaschke, F. (2019), How many solar wind data are sufficient for accurate fluxgate magnetometer offset determinations?, Geoscientific Instrumentation Methods and Data Systems, 8(2), 285-291, doi:10.5194/gi-8-285-2019.

Pope, S. A., Zhang, T. L., Balikhin, M. A., Delva, M., Hvizdos, L., Kudela, K., et al. (2011), Exploring planetary magnetic environments using magnetically unclean spacecraft: a systems approach to VEX MAG data analysis, Annales Geophysicae, 29(4), 639-647, doi:10.5194/angeo-29-639-2011.

Pudney, M. A., Carr, C. M., Schwartz, S. J., & Howarth, S. I. (2012), Automatic parameterization for magnetometer zero offset determination, Geoscientific Instrumentation Methods and Data Systems, 1(2), 103-109, doi:10.5194/gi-1-103-2012.

Risbo, T., Brauer, P., Merayo, J. M. G., Nielsen, O. V., Petersen, J. R., Primdahl, F., et al. (2003), Orsted pre-flight magnetometer calibration mission, Measurement Science and Technology, 14(5), 674-688, doi:10.1088/0957-0233/14/5/319.

Russell, C. T., Anderson, B. J., Baumjohann, W., Bromund, K. R., Dearborn, D., Fischer, D., et al. (2016), The Magnetospheric Multiscale Magnetometers, Space Science Reviews, 199(1-4), 189-256, doi:10.1007/s11214-014-0057-3.

Schmid, D., Plaschke, F., Narita, Y., Heyner, D., Mieth, J. Z. D., Anderson, B. J., Volwerk, M., Matsuoka, A., & Baumjohann, W. (2020), Magnetometer in-flight offset accuracy for the BepiColombo spacecraft, Annales Geophysicae, 38(4), 823-832, doi:10.5194/angeo-38-823-2020.

Shan, L. C., Lu, Q. M., Mazelle, C., Huang, C., Zhang, T. L., Wu, M. Y., et al. (2015), The shape of the Venusian bow shock at solar minimum and maximum: Revisit based on VEX observations, Planetary and Space Science, 109, 32-37, doi:10.1016/j.pss.2015.01.004.

https://doi.org/10.5194/angeo-2021-46
Preprint. Discussion started: 17 August 2021

Annales Geophysicae Discussions

Titov, D. V., Svedhem, H., Koschny, D., Hoofs, R., Barabash, S., Bertaux, J. L., et al. (2006), Venus express science planning, Planetary and Space Science, 54(13-14), 1279-1297, doi:10.1016/j.pss.2006.04.017.

Volwerk, M., Mautner, D., Wedlund, C. S., Goetz, C., Plaschke, F., Karlsson, T., et al. (2021), Statistical study of linear magnetic hole structures near Earth, Annales Geophysicae, 39(1), 239-253, doi:10.5194/angeo-39-239-2021.

Wang, G. Q., Ge, Y. S., Zhang, T. L., Nakamura, R., Volwerk, M., Baumjohann, W., et al. (2015), A statistical analysis of Pi2-band waves in the plasma sheet and their relation to magnetospheric drivers, Journal of Geophysical Research: Space Physics, 120(8), 6167-6175, doi:10.1002/2014ja020753.

Wang, G. Q., Zhang, T. L., & Volwerk, M. (2016), Statistical study on ultralow-frequency waves in the magnetotail lobe observed by Cluster, Journal of Geophysical Research-Space Physics, 121(6), 5319-5332, doi:10.1002/2016ja022533.

Wang, G. Q., Volwerk, M., Zhang, T. L., Schmid, D., & Yoshikawa, A. (2017), High-latitude Pi2 pulsations associated with kink-like neutral sheet oscillations, Journal of Geophysical Research: Space Physics, 122(3), 2889-2899, doi:10.1002/2016ja023370.

Wang, G. Q., Volwerk, M., Xiao, S. D., Wu, M. Y., Hao, Y. F., Liu, L. J., et al. (2020), Three-dimensional Geometry of the Electron-scale Magnetic Hole in the Solar Wind, Astrophysical Journal Letters, 904(1), doi:10.3847/2041-8213/abc553.

Wang, G. Q., & Pan, Z. H. (2021), A New Method to Calculate the Fluxgate Magnetometer Offset in the Interplanetary Magnetic Field, Journal of Geophysical Research: Space Physics, 126(4), doi:10.1029/2020ja028893.

Wang, G. Q., Volwerk, M., Wu, M. Y., Hao, Y. F., Xiao, S. D., Wang, G., et al. (2021a), First Observations of an Ion Vortex in a Magnetic Hole in the Solar Wind by MMS, The Astronomical Journal, 161(3), doi:10.3847/1538-3881/abd632.

Wang, G. Q., Zhang, T. L., Wu, M. Y., Xiao, S. D., Wang, G., Chen, Y. Q., et al. (2021b), Field-Aligned Currents Originating From the Chaotic Motion of Electrons in the Tilted Current Sheet: MMS Observations, Geophysical Research Letters, 48(9), doi:10.1029/2020gl088841.

Wu, D. J., Feng, H. Q., Li, B., & He, J. S. (2016), Nature of turbulence, dissipation, and heating in space plasmas: From Alfvén waves to kinetic Alfvén waves, Journal of Geophysical Research: Space Physics, 121(8), 7349-7352, doi:10.1002/2016ja023082.

Xiao, S. D., Wu, M. Y., Wang, G. Q., Wang, G., Chen, Y. Q., & Zhang, T. L. (2020a), Turbulence in the near-Venusian space: Venus Express observations, Earth and Planetary Physics, 4(1), 1-6, doi:10.26464/epp2020012.

Xiao, S. D., Zhang, T. L., Vörös, Z., Wu, M. Y., Wang, G. Q., & Chen, Y. Q. (2020b), Turbulence Near the Venusian Bow Shock: Venus Express Observations, Journal of Geophysical Research-Space Physics, 125(2), doi:10.1029/2019JA027190.

Zhang, T. L., Baumjohann, W., Delva, M., Auster, H. U., Balogh, A., Barabash, S., et al. (2006), Magnetic field investigation of the Venus plasma environment: Expected new results from Venus Express, Planetary and Space Science, 54(13-14), 1336-1343, doi:10.1016/j.pss.2006.04.018.

Annales Geophysicae
Open Access
Discussions

Zhang, T. L., Lu, Q. M., Baumjohann, W., Russell, C. T., Fedorov, A., Barabash, S., et al. (2012), Magnetic reconnection in the near Venusian magnetotail, Science, 336(6081), 567-570, doi:10.1126/science.1217013.